J Porous Mater (2017) 24:121–128
DOI 10.1007/s10934-016-0244-6

Preparation and properties of alumina foams via thermally induced foaming of molten D-glucose monohydrate

Keke Huang[1] · Yuanbing Li[1] · Shujing Li[1] · Ruofei Xiang[1]

Published online: 12 July 2016
© Springer Science+Business Media New York 2016

Abstract Alumina foams with porosity of 92.6–94.4 % were obtained by thermally induced foaming of powder dispersions in molten D-glucose monohydrate. Effects of alumina to D-glucose monohydrate weight ratio on the preparation and properties of the alumina foams were investigated. The bubbles generated in molten D-glucose monohydrate were stabilized by alumina particles adsorbed at the gas–liquid interface and the increase in viscosity of the dispersions. The foam rise decreased with the increase in alumina to D-glucose monohydrate weight ratio up to 1.2 and then slightly increased. The alumina foams showed cellular microstructure and the cells had a near spherical morphology. Increasing alumina to D-glucose monohydrate weight ratio widened the cell and window size distribution. The density and compressive strength of the alumina foam showed a maximum at alumina to D-glucose monohydrate weight ratio of 1.2. The corresponding maximum density and compressive strength were 0.293 g/cc and 1.14 MPa, respectively.

Keywords Alumina · Foams · Microstructure · Pore distribution · Compressive strength

1 Introduction

Porous alumina ceramics have many properties including good chemical stability, high refractoriness, low density, low thermal conductivity and high surface area [1–3], which make them useful for applications such as catalyst supports [4], filters [5], and biomedical implants [6], thermal insulation [7].

Several methods have been employed to fabricate porous alumina ceramics, including polymeric foam impregnation [8], direct foaming [9], gel casting [10], and so on. The most common process for producing ceramic foams is the polymeric foam impregnation, which consists in the impregnation of a flexible polymeric sponge with a ceramic slurry, the removal of excess slip by squeezing or centrifuging, followed by drying, a burn-out step to eliminate the polymer template and high-temperature sintering [11]. However, alumina foams produced by this technique are of low strength because (1) they usually contain a central hole and (2) the struts are likely to contain cracks [12]. In case of direct foaming technique, a ceramic suspension is foamed by gas incorporation; the wet foam is stabilized, dried, and sintered. Wet foams are thermodynamically unstable systems in which processes like drainage of the liquid phase and gas bubble coarsening lead to foam degradation and final destruction. Surfactants are usually used as surface-active agents for the stabilization of wet foams. In gel casting, a ceramic powder suspension containing organic monomer and cross linking agent is foamed by using a blowing agent followed by setting by in situ polymerization of the monomer [13]. The method produces porous ceramics with small pore sizes and also gives relatively high mechanical strength [14]. However, alumina foams derived from this method often use monomers and surfactant molecules as the processing additives. Some additives such as acrylamide are reported to be toxic [15, 16].

The processing methods mentioned above to prepare alumina foams often use synthetic organic polymers and monomers, surfactant molecules and solvents, which are

✉ Yuanbing Li
lybref2002@126.com

[1] The State Key Laboratory of Refractories and Metallurgy, Wuhan University of Science and Technology (WUST), Wuhan 430081, People's Republic of China

produced from petroleum. Replacement of petroleum based raw materials with non-toxic natural renewable resources for the preparation of alumina foams is very important for sustainable development. Recently, natural renewable materials such as proteins, polysaccharides, sucrose, and yeast have been studied for the preparation of alumina foams [17–20]. Fey et al. [21] used agarose as gelling agent for the fabrication of alumina gel-cast foams. Sucrose was used as binder and rheology modifier during wet processing of porous alumina ceramics [22]. Sucrose used as binder as well as a pore former in dry processing to produce porous alumina ceramics was also reported [19]. Caramelization commonly occurs when sugars are heated, either dry or in concentrated solution, either alone or with certain additives [23]. Caramelization of glucose is the process of removal of water produced by the condensation reactions followed by isomerization and polymerization steps. Once the bubbles generated in the molten D-glucose monohydrate due to the water vapor produced by the condensation reactions are stabilized by alumina particles, the method can be used for the preparation of porous alumina ceramics. In this process, D-glucose monohydrate–alumina powder mixtures were heated to obtain alumina powder dispersions in molten D-glucose monohydrate. The foaming and setting of the dispersions were carried out by heating at 130 °C in an air oven to form green foam bodies. The alumina foams with high porosity in the range of 92.6–94.4 % were prepared by sintering of the green foam bodies at 1600 °C. The molten D-glucose monohydrate based process expects to have several advantages compared to the methods mentioned above. Alumina foams prepared by the molten D-glucose monohydrate based process have a uniform structure and avoid vast hollow struts, which is in contrast to that obtained by polymeric foam impregnation. The molten D-glucose monohydrate based process avoids the harmful additives such as synthetic organic polymers and monomers. Also, D-glucose monohydrate is nontoxic, biodegradable, cheap, and widely available. Effects of alumina to D-glucose monohydrate weight ratio on dispersion and foaming characteristics of dispersions such as viscosity, foam rise, properties such as density, porosity, cell size, cell window size, sintering shrinkage and compressive strength were investigated.

2 Experimental procedure

2.1 Materials

α-Alumina powder (Kaifeng Special Refractories Co., Ltd., China, $d_{50} = 2.37$ μm) and analytical reagent grade D-glucose monohydrate (CAS NO: 5996-10-1, Sinopharm Chemical Reagent Co., Ltd., China.) were used as raw materials.

2.2 Preparation of alumina powder dispersions in molten monohydrate

Dispersions were first prepared by mixing powders for 4 h in a polyurethane bottle rotating at a speed of 400 rev/min with corundum balls as the abrasive media, which are composed by the alumina and D-glucose monohydrate (80 g) with various weight ratios (0.8, 1.0, 1.2 and 1.4), then the well mixed D-glucose monohydrate–alumina powder mixtures were placed in a mold at 195 °C to melt the D-glucose monohydrate. After 2 min of stirring with a glass rod, the homogeneous alumina powder dispersions in molten D-glucose monohydrate were obtained.

2.3 Preparation of ceramics foams

The dispersions were heated in an air oven at 130 °C for foaming and setting. After demolding, the green foam bodies were cut into rectangular bodies and then sintered at 1600 °C for 3 h in air atmosphere. The heating rates used were 1 and 2 °C/min from room temperature to 550 °C and from 550 to 1600 °C, respectively. The flow chart for the preparation of alumina foams is shown in Fig. 1.

2.4 Characterization

Particle size was measured by Laser Particle Size Analyzer (Mastersizer 2000, Malvern Instruments Ltd., UK). The viscosity of the alumina powder dispersions in molten D-glucose monohydrate was measured at 130 °C using a rheometer (MCR 301 Anton Paar Physics, Germany) with a cylindrical spindle (CC17-SN28332) measurement system. The foaming capacity of dispersions was evaluated by measuring the change in volume of dispersions. 15 mL dispersions contained in a 100 mL meter glass was placed at 130 °C in an air oven for foaming and setting. The foam rise was calculated as the ratio of the final volume of the foam and the initial volume of the dispersion. The average foam rise represented an average of three measurements for each alumina to D-glucose monohydrate weight ratio. The density of alumina foams was calculated by mass and dimension at a minimum of five samples with regular shapes. The theoretical density of fully densified alumina (3.98 g/cc) was used as a reference to calculate the total volume fraction of porosity. The volume shrinkage of samples was calculated from the initial and final dimensions. Five samples were used to get the average volume shrinkage. The compressive strength of the samples was examined using a universal testing machine (ETM, Wance, China) at a crosshead speed of 0.5 mm/min with 40 mm × 40 mm × 15 mm samples (ASTM standard C365/C365M-05). Each value represented an average of five measurements of five different samples. Microstructures of the

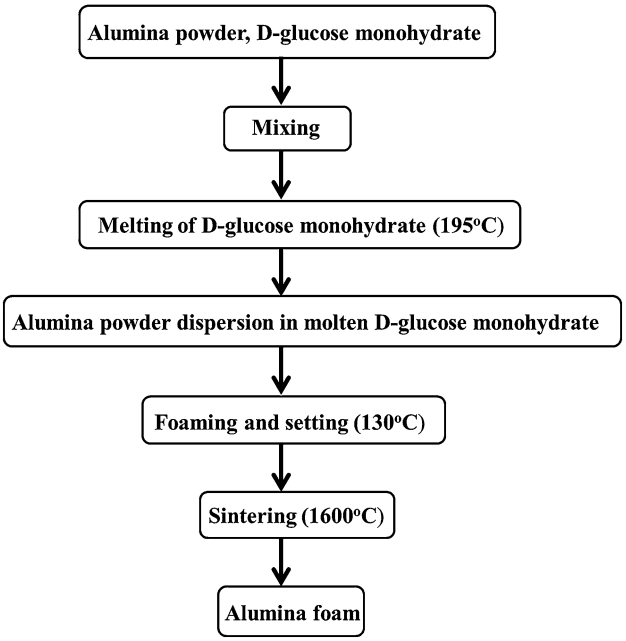

Fig. 1 Flow chart for the preparation of alumina foams

sintered samples were observed with a field emission scanning electron microscope (SEM, JSM-6610, JEOL, Japan) on fracture surfaces and the cross sections of resin infiltrated samples. The SEM samples were coated with gold to prevent charging effect. In order to determine the cell size, cell window size and strut thickness of the alumina foams, SEM image of the cross sections of resin infiltrated samples were analyzed after binaryzation using a micro-image analysis and process program (MIAPS, Precise, China). In binaryzation images, all pores were submerged in the infiltrated resin showed as the green color and only bright dense alumina struts were intersected between them. The diameters of the cells and the windows were taken as cell sizes as well as window sizes respectively. The sizes of over 500 cells and windows were measured and Fig. 2a shows parts of the measurements. The thicknesses of approximate 67 struts were measured, and Fig. 2b shows a few strut thickness measurements on a micrograph.

3 Results and discussion

3.1 Dispersion and foaming characteristics of alumina powders in molten D-glucose monohydrate

The viscosity at various shear rates of the alumina powder dispersions in molten D-glucose monohydrate were measured at 130 °C. Figure 3 shows the influence of alumina to D-glucose monohydrate weight ratio on the viscosity of the alumina powder dispersions in molten D-glucose monohydrate. The molten D-glucose monohydrate without alumina addition showed viscosity in the range of 0.55–0.64 Pa s at shear rates in the range of 1–200 s^{-1}. The alumina powder dispersions in molten D-glucose monohydrate showed shear thinning character. The viscosity and shear thinning character of the alumina powder dispersions in molten D-glucose monohydrate increased with the increase in alumina to D-glucose monohydrate weight ratio. The viscosity of the alumina powder dispersions in D-glucose monohydrate depend on the intermolecular forces [24]. Hydrogen bonding and Van der Waals forces exist in D-glucose monohydrate, while Van der Waals forces exist between alumina particles. It is well known that the particles in a powder dispersion experience an interparticle attractive interaction due to the Van der Waals forces [24]. This Van der Waals interaction increases with an increase in the powder loading [24]. The increase in viscosity and shear thinning character of alumina powder dispersions with the increase in alumina concentration may be resulted from the increase in the interparticle interactions.

The foaming of molten D-glucose monohydrate includes the formation of glucosan (1,2-anhydro-α-D-glucose) and levoglucosan (1,6-anhydro-β-D-glucose) followed by their condensation through the hydroxyl groups to form 5-hydroxymethyl-2-furfural [23, 25]. Bubbles generated in the molten D-glucose monohydrate due to the water vapor produced by the condensation reactions may be stabilized by two mechanisms. The stabilization of bubbles in a liquid medium can be achieved by increasing the viscosity of the liquid to a sufficiently higher value [26]. It has been observed that foams obtained by the foaming of the molten D-glucose monohydrate without alumina powders are stable until setting into solid. In the present case, the bubbles may be stabilized against coalescence and rupture due to the higher viscosity of the molten D-glucose monohydrate in presence of alumina powders. Moreover, the liquid D-glucose monohydrate gradually transformed to a solid through condensation reactions during the foaming of alumina powder dispersions, leading to the increase in viscosity of the dispersions and prohibiting the growth and movement of bubbles. Thus, the bubbles may be stabilized by the relative high initial viscosity and rapid increase in viscosity of alumina powder dispersions in molten D-glucose monohydrate. Particles in the correct size range and with the appropriate wetting properties can become essentially irreversibly adsorbed [27]. Stabilization of bubbles by particles has been reported for the foaming of powder suspensions [28, 29]. In the present case, the bubbles may also be stabilized by alumina particles adsorbed at the gas–liquid interface.

Figure 4 illustrates the effect of alumina to D-glucose monohydrate weight ratio on the foam rise (a measure of

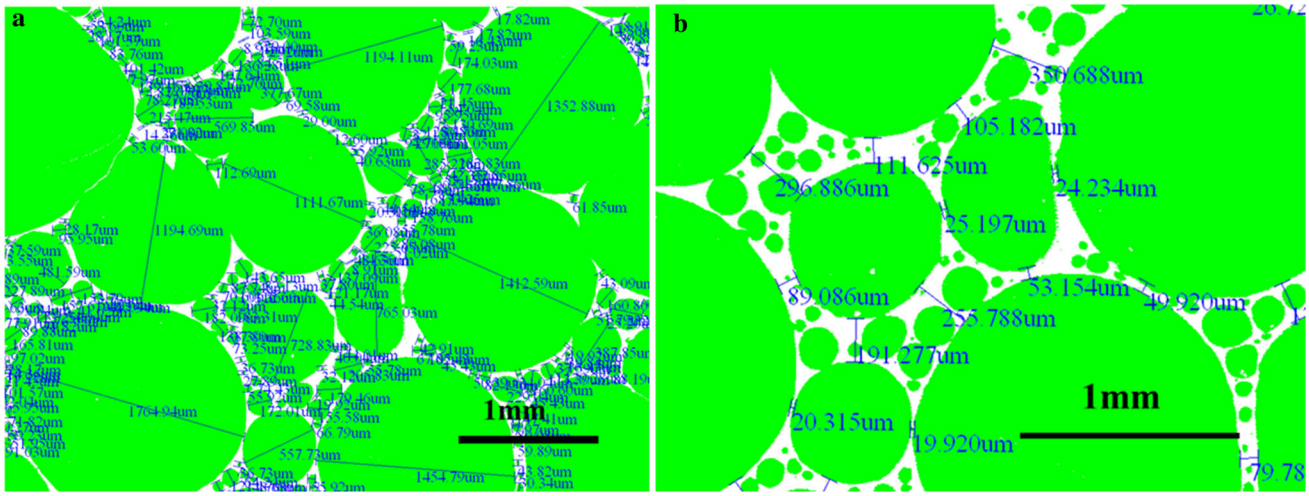

Fig. 2 **a** Cell and window size measurements, and **b** strut thickness measurements

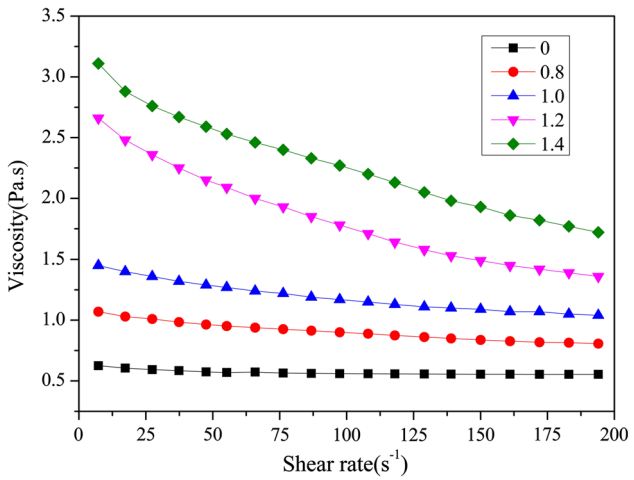

Fig. 3 Viscosity versus shear rate of the alumina powder dispersions at various alumina to D-glucose monohydrate weight ratios at 130 °C

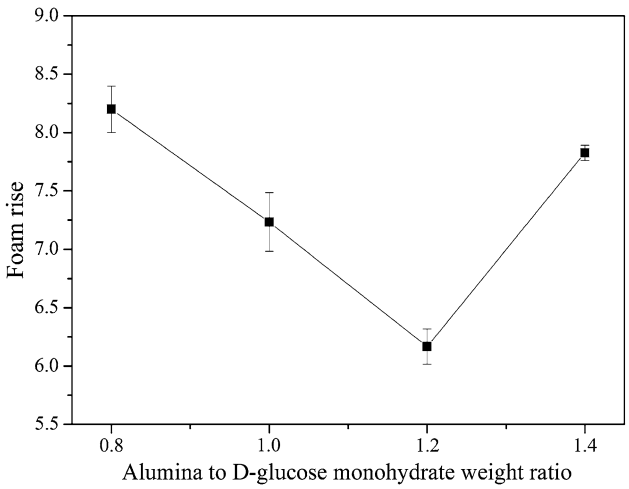

Fig. 4 Effect of alumina to D-glucose monohydrate weight ratio on the foam rise

foam volume). The foam rise of the foam samples declined from 8.2 to 6.2 when alumina to D-glucose monohydrate weight ratio increased from 0.8 to 1.2. A further increase in alumina to D-glucose monohydrate weight ratio to 1.4 slightly increased the foam rise value to 7.8. In this study, the foam volume was greatly dependent on the number of bubbles and bubble sizes. Generally, the increase in number of bubbles and bubble sizes is beneficial to increase the foam rise. The higher D-glucose monohydrate concentrations, the larger numbers of bubbles nucleated from gas molecules (water vapor) generated in molten D-glucose monohydrate. Therefore, the decrease in D-glucose monohydrate concentration reduced the number of bubbles, which may be mainly responsible for the decline in foam rise from 8.2 to 6.2. Though there was a decrease in the number of bubbles, the foam rise increased when the alumina to D-glucose monohydrate weight ratio increased to 1.4. The increase in alumina concentration not only increased the viscosity but also increased the alumina particles coverage on the bubble surface, which benefited the bubble stability. Thus, the higher viscosity of alumina powder dispersions in molten D-glucose monohydrate had positive effects on the growth of bubbles that resulted in larger cells, which led to the increase in foam rise. Wang and Shi also reported that cell size of aluminum foam increased with increasing ceramic particle concentration [30].

3.2 Microstructure and mechanical properties of alumina foams

The fracture morphology of the sintered foams is shown in Fig. 5a–d. The foam showed cellular microstructure. There

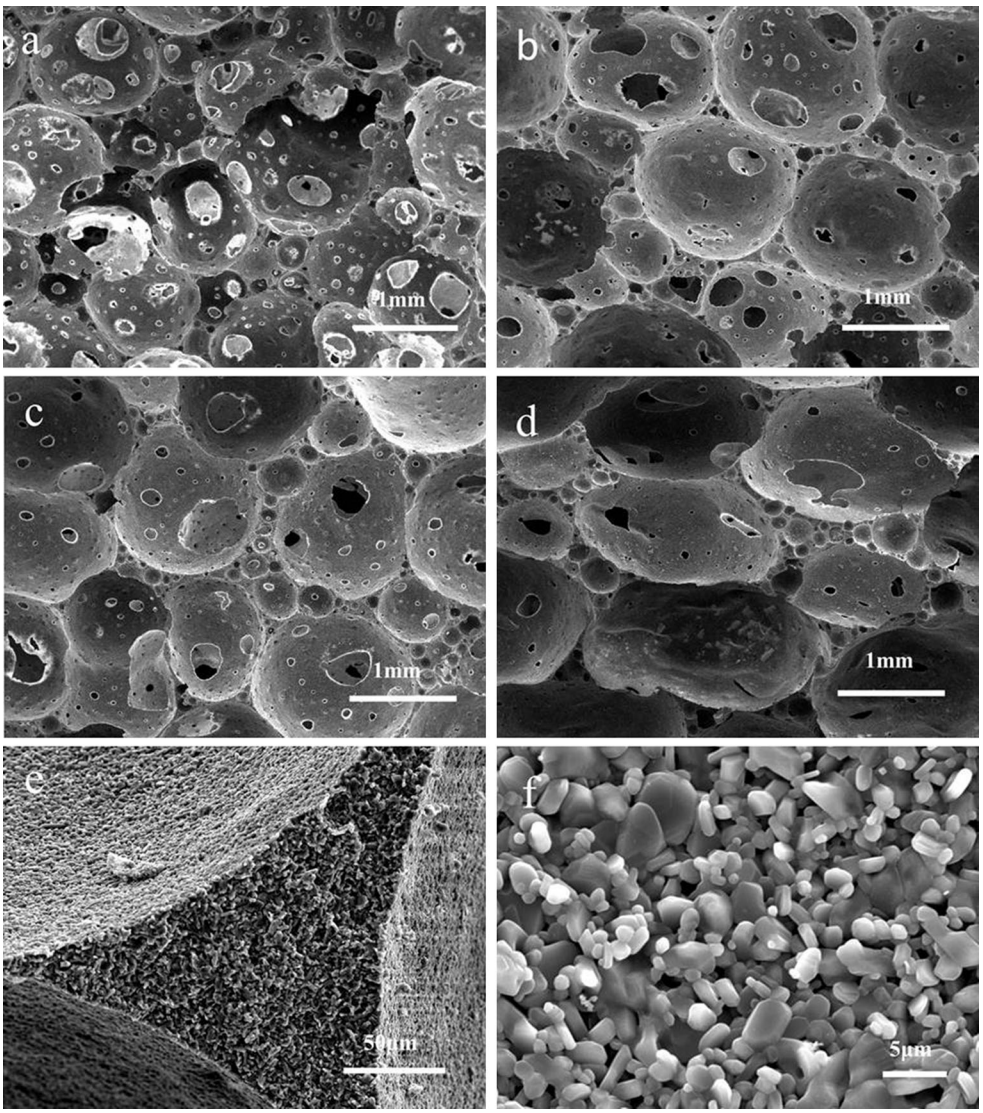

Fig. 5 Morphology of alumina foams at various alumina to D-glucose monohydrate weight ratios: **a** 0.8, **b** 1.0, **c** 1.2, **d** 1.4, **e** detail of a strut, **f** the cell wall

were two noticeable pore types: i.e. the large spherical cells and the small windows on the walls of spherical cells. It has been observed that alumina foams prepared by the molten D-glucose monohydrate based process had a uniform structure. Additionally, the alumina foams prepared by the molten D-glucose monohydrate based process had no vast hollow struts, as shown in Fig. 5e. At the alumina to D-glucose monohydrate weight ratio of 1.4 there was a large deformation of the spherical cell morphology. The deformation resulted in the near oval shaped cells. As the alumina concentration increased, the molten D-glucose monohydrate layer thickness around the alumina particle decreased. When the layer thickness was less than a certain value, the particle to particle contact established that acted as a weak point which led to the rupture of the bubbles before setting. The partial foams collapse caused the large deformation of the spherical cell morphology. As seen in Fig. 5f, the foam had dense strut and close packed alumina grains on the cell wall surface.

The cell size and window size increased with increasing the alumina to D-glucose monohydrate weight ratios. At an alumina to D-glucose monohydrate weight ratio of 0.8, foams exhibited a cell size of 482–1451 μm and window size of 14–457 μm. When an alumina to D-glucose monohydrate weight ratio was 1.0, the cell and window size increased to 494–1579 μm and 18–462 μm, respectively. At a higher alumina to D-glucose monohydrate weight ratio (1.2) both pore types were presented with a cell size of 590–1665 μm and window size of 20–550 μm. With alumina to D-glucose monohydrate weight ratio increased to

1.4, foams showed a cell size of 663–3056 μm and window size of 17–562 μm. It could be seen that increasing the alumina content widened the cell and window size distribution. The increase in cell and window size may be due to the enhanced bubble stabilization by the increased adsorption of alumina particles at the gas–liquid interface. The rapid increase in viscosity at higher alumina concentration also provides additional bubble stability that result in larger cell and window size. The cell and window size distribution of sintered foams obtained from various alumina to D-glucose monohydrate weight ratios are illustrated in Fig. 6.

At an alumina to D-glucose monohydrate weight ratio of 0.8, the foams exhibited a narrow distribution ($d_{10} = 429$ μm, $d_{50} = 782$ μm and $d_{90} = 1168$ μm) with a small mean cell size of 900 μm. Increasing the alumina to D-glucose monohydrate weight ratio to 1.0 mean cell size increased to 959 μm and cell size distribution exhibited a wider distribution ($d_{10} = 416$ μm, $d_{50} = 707$ μm and $d_{90} = 1484$ μm). Further increasing the alumina to D-glucose monohydrate weight ratio to1.2 mean cell size increased to 1098 μm and also cell size distribution was increasing to $d_{10} = 549$ μm, $d_{50} = 757$ μm and $d_{90} = 1471$ μm. The widest cell size distribution of $d_{10} = 536$ μm, $d_{50} = 1295$ μm and $d_{90} = 2476$ μm as well as the highest mean cell size of 1524 μm was measured for foams at an alumina to D-glucose monohydrate weight ratio of 1.4. Regarding to the unimodal cell window size distribution the foams exhibited a narrow distribution (mean 89–111 μm) with less difference among various alumina to D-glucose monohydrate weight ratios.

The main geometrical parameters of the foams: density, porosity, sintering shrinkage, mean cell size, mean cell window size and mean strut thickness are given in Table 1. The total volume shrinkage of the foam samples during the polymer burnout and sintering decreased from 62.5 to 48 % when the alumina to D-glucose monohydrate weight ratio increased from 0.8 to 1.4. Samples prepared at an alumina to D-glucose monohydrate weight ratio of 0.8 showed slightly higher density in spite of its lower alumina concentration compared to that prepared at an alumina to D-glucose monohydrate weight ratio of 1.0. The higher density is mainly owing to the large volume shrinkage. When the weight ratio of alumina to D-glucose monohydrate increased to 1.4, the density decreased to 0.287 g/cc. This decrease may occur from the large foam volume and small volume shrinkage. The corresponding porosity values were in the range from 92.6 to 94.4 %.

The mean strut thickness increased with the increase in alumina to D-glucose monohydrate weight ratios, as shown in Table 1. The presence of alumina particles in the D-glucose monohydrate melt increases the viscosity of the dispersions, and the higher viscosity slows down liquid flow and thus retards the cell wall drainage before it solidifies. Apart from their influence on the viscosity of the dispersions, the alumina particles have an important impact on foam stability through their attachment to the gas–liquid interface. The increase in the cell thickness suggests that the viscosity of the dispersions is becoming higher and higher as more alumina particles are incorporated into the dispersions. Moreover, the increase in cell wall thickness also means that more aggregation of particles in the dispersions creates more tortuous paths for the liquid and acts as a liquid flow barrier from the cell wall towards the plateau border. As a result, the cell wall drainage is retarded, resulted in the increase in cell wall thickness.

Figure 7 shows the effect of alumina to D-glucose monohydrate weight ratio on the compressive strength. It is well recognized that foam mechanical properties are influenced by the properties of the base material, relative

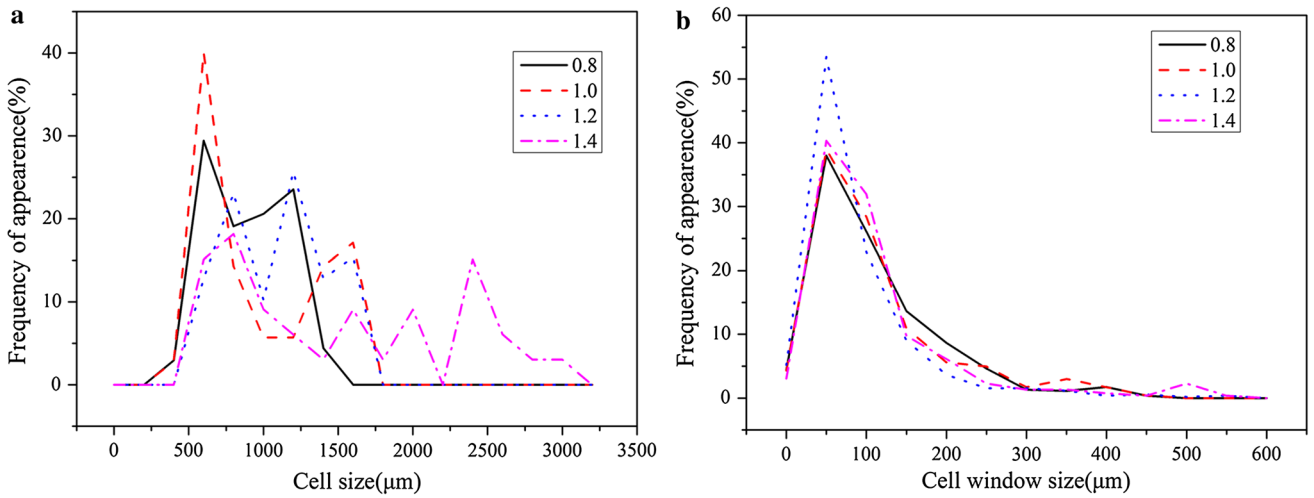

Fig. 6 Cell and window size distribution of sintered foams obtained from various alumina to D-glucose monohydrate weight ratios

Table 1 Effect of alumina to D-glucose monohydrate weight ratio on the density, porosity, sintering shrinkage, cell size, cell window size and strut thickness of alumina foams

Alumina to D-glucose monohydrate weight ratio	Density (g/cc)	Porosity (%)	Sintering shrinkage (vol%)	Mean cell size (μm)	Mean cell window size (μm)	Mean strut thickness (mm)
0.8	0.237 ± 0.007	94.0 ± 0.2	62.5 ± 0.6	900 ± 276	111 ± 83	158 ± 92
1.0	0.224 ± 0.003	94.4 ± 0.1	56.1 ± 0.4	959 ± 397	112 ± 88	184 ± 112
1.2	0.293 ± 0.006	92.6 ± 0.1	52.1 ± 0.3	1098 ± 325	86 ± 79	198 ± 140
1.4	0.287 ± 0.003	92.8 ± 0.1	48.0 ± 0.9	1525 ± 765	111 ± 97	210 ± 122

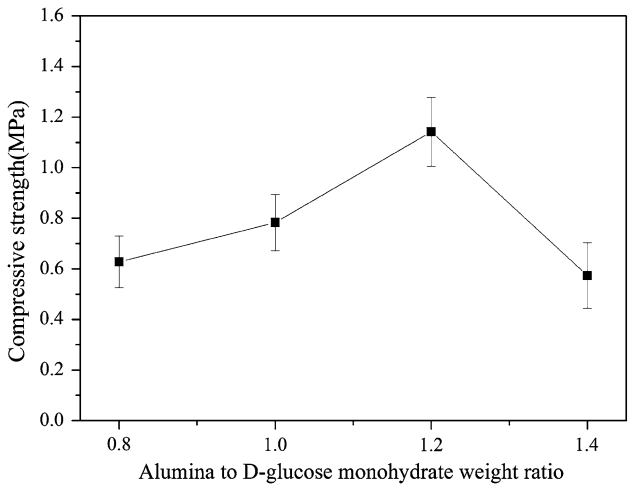

Fig. 7 Effect of alumina to D-glucose monohydrate weight ratio on compressive strength

density (ratio of the foam density to the density of base material) and microstructural geometry. The compressive strength of brittle foams is related to density, cell size and structure of the strut [31, 32]. Generally, the compressive strength increased with the increase in foam density, the increase in strut thickness and the decrease in cell size. Though there was an increase in cell size, the compressive strength of samples increased from 0.63 to 1.14 MPa when alumina to D-glucose monohydrate weight ratio increased from 0.8 to 1.2. This could be attributed to the increase in density and strut thickness. A further increase in alumina to D-glucose monohydrate weight ratio of 1.4 caused a remarkable decrease in compressive strength. This may be resulted from the decrease in density, the large cell size and the deformation of spherical cells.

4 Conclusions

The molten D-glucose monohydrate based process enabled the fabrication of alumina foams without using any synthetic organic materials as processing additives. Cellular alumina foams with porosity in the range of 92.6–94.4 % were fabricated by thermally induced foaming of alumina powder dispersions in molten D-glucose monohydrate that exhibited shear thinning character. The viscosity of the dispersions could be tailored by adjusting the weight ratio of alumina to D-glucose monohydrate. The bubbles were stabilized by alumina particles adsorbed at the gas–liquid interface and the increase in viscosity of the dispersions. The foam rise decreased with increase in alumina to D-glucose monohydrate weight ratio up to 1.2 and then slightly increased. With alumina to D-glucose monohydrate weight ratio increasing, cell size and strut thickness increased. The density and compressive strength of the alumina foam showed a maximum at alumina to D-glucose monohydrate weight ratio of 1.2. The corresponding maximum density and compressive strength were 0.293 g/cc and 1.14 MPa, respectively.

References

1. A.R. Studart, U.T. Gonzenbach, E. Tervoort, L.J. Gauckler, J. Am. Ceram. Soc. **89**, 1771–1789 (2006)
2. X.M. Li, M.J. Gao, Y. Jiang, Ceram. Int. **42**, 12531–12535 (2016)
3. X.M. Li, P.T. Wu, D.L. Zhu, Int. J. Refract. Met. Hard Mater. **41**, 437–441 (2013)
4. R. Faure, F. Rossignol, T. Chartier, C. Bonhommea, A. Maître, G. Etchegoyen, P.D. Gallo, D. Gary, J. Eur. Ceram. Soc. **31**, 303–312 (2011)
5. M.W. Kennedy, K.X. Zhang, R. Fritzsch, S. Akhtar, J.A. Bakken, R.E. Aune, Metall. Mater. Trans. B **44B**, 671–690 (2013)
6. B.H. Yoon, W.Y. Choi, H.E. Kim, J.H. Kim, Y.H. Koh, Scr. Mater. **58**, 537–540 (2008)
7. J.J. Liu, Y.B. Li, Y.W. Li, S.B. Sang, S.J. Li, Ceram. Int. **42**, 8221–8228 (2016)
8. J. Luyten, I. Thijs, W. Vandermeulen, S. Mullens, B. Wallaeys, R. Mortelmans, Adv. Appl. Ceram. **104**, 4–8 (2005)
9. U.T. Gonzenbach, A.R. Studart, E. Tervoort, L.J. Gauckler, J. Am. Ceram. Soc. **90**, 16–22 (2007)
10. A.C. Young, O.O. Omatete, M.A. Janney, P.A. Menchhofer, J. Am. Ceram. Soc. **74**, 612–618 (1991)
11. P. Colombo, Phil. Trans. R. Soc. A **364**, 109–124 (2006)
12. S.N. Jayasinghe, M.J. Edirisinghe, J. Porous Mater. **9**, 265 (2002)
13. K. Prabhakaran, A. Melkeri, N.M. Gokhale, S.C. Sharma, Ceram. Int. **33**, 77–81 (2007)
14. J.H. Lee, H.J. Choi, S.Y. Yoon, B.K. Kim, H.C. Park, J. Porous Mater. **20**, 219–220 (2013)
15. F.S. Ortega, P. Sepulveda, V.C. Pandolfelli, J. Eur. Ceram. Soc. **22**, 1395–1401 (2002)

16. X.G. Deng, J.K. Wang, J.H. Liu, H.J. Zhang, F.L. Li, H.J. Duan, L.L. Lu, Z. Huang, W.G. Zhao, S.W. Zhang, Ceram. Int. **41**, 9009–9017 (2015)
17. S. Dhara, P. Bhargava, J. Am. Ceram. Soc. **84**, 3048–3050 (2001)
18. F.S. Ortega, F.A.O. Valenzuela, C.H. Scuracchio, V.C. Pandolfelli, J. Eur. Ceram. Soc. **23**, 75–80 (2003)
19. K. Mohanta, A. Kumar, O. Parkash, D. Kumar, J. Eur. Ceram. Soc. **34**, 2401–2412 (2014)
20. T. Uhlířová, E. Gregorová, W. Pabst, V. Němcina, J. Eur. Ceram. Soc. **35**, 187–196 (2015)
21. T. Fey, B. Zierath, P. Greil, M. Potoczek, J. Porous Mater. **22**, 1305–1312 (2015)
22. M. Pradhan, P. Bhargava, J. Am. Ceram. Soc. **88**, 216–218 (2005)
23. V. Ratsimba, J.M. Garćıa Fernández, J. Defaye, H. Nigay, A. Voilley, J. Chromatogr. A **844**, 283–293 (1999)
24. G.D. Parfitt, in Fundamental Aspects of Dispersion, ed. By G.D. Parfitt (Applied Science, NJ, 1981), pp. 1–47
25. J.M. deMan, *Principles of food chemistry*, 3rd edn. (Chapman & Hall, Maryland, 1999), p. 175
26. G. Rosebrock, A. Elgafy, T. Beechem, K. Lafdi, Carbon **43**, 3075–3087 (2005)
27. B.S. Murray, Stabilization of bubbles and foams. Curr. Opin. Colloid Interface Sci. **12**, 237 (2007)
28. U.T. Gonzenbach, A.R. Studart, D. Steinlin, E. Tervoort, L.J. Gauckler, J. Am. Ceram. Soc. **90**, 3407–3414 (2007)
29. V. Sciamanna, B. Nait-Ali, M. Gonon, Ceram. Int. **41**, 2599–2606 (2015)
30. D.Q. Wang, Z.Y. Shi, Mater. Sci. Eng. A **361**, 45–49 (2003)
31. F.A.C. Oliveira, S. Dias, M.F. Vaz, J.C. Fernandes, J. Eur. Ceram. Soc. **26**, 179–186 (2006)
32. M.F. Ashby, Metall. Trans. A **14A**, 1755–1769 (1983)